Key Engineering Materials
ISSN: 1662-9795, Vol. 926, pp 1248-1256
doi:10.4028/p-165q46

Submitted: 2021-12-03
Revised: 2022-01-17
Accepted: 2022-02-18
Online: 2022-07-22

Simulation of Wrinkling during Forming of Binder Stabilized UD-NCF Preforms in Wind Turbine Blade Manufacturing

Peter Hede Broberg[1,2,a*], Christian Krogh[1,b], Esben Lindgaard[1,2,c], and Brian Lau Verndal Bak[1,2,d]

[1]Department of Materials and Production, Aalborg University, Fibigerstraede 16, Aalborg, Denmark

[2] CraCS Research group, Aalborg University, www.CraCS.aau.dk

[a]phb@mp.aau.dk, [b]ck@mp.aau.dk, [c]elo@mp.aau.dk, [d]brianbak@mp.aau.dk

Keywords: Forming simulation, Dry-binder preforms, Non-crimp fabrics, Wrinkles

Abstract. Binder stabilized preforms are getting increased attention in the wind turbine industry with the aim to increase automation in the production of large blades. In this context a preform is a stack of dry unidirectional glass fiber non-crimp fabrics (UD-NCF), which is consolidated using a polymeric binder. The preform is manufactured in a separate mold, and subsequently placed in the main blade mold. During placement of preforms, fiber wrinkling may occur due to the deformation of the preform. To accommodate this problem, we propose a predictive simulation model that can be used to investigate how different process parameters influence the wrinkle creation. Most forming simulation models in the literature consider frictional laws in the inter-ply interface for multi-layered fabrics. In this work the binder interfaces between the layers are modelled using a cohesive traction-separation law to accurately model binder degradation and wrinkle creation during preform deformation. The model predictions are compared with full thickness preform coupon specimens.

Introduction

To cut down on production cost of large wind turbine blades the use of binder stabilized preforms may be used to increase automation and decrease process times. Binder stabilized preforms are stacks of dry unidirectional glass fiber non-crimp fabrics (UD-NCF) which are pre-consolidated with a polymeric binder, prior to placement in the main blade mold. Wrinkling may occur at geometric transitions during placement of the preforms in the blade mold. This happens because the binder impedes relative ply sliding, which lead to excessive ply length at geometric transitions. These fiber wrinkles may cause a severe knockdown on the wind turbine blade strength [1].

Simulation models may be used to predict fiber wrinkling during different manufacturing steps. They can, generally, be divided into kinematic and mechanical models. Kinematic models are computational efficient [2], but are not capable of describing the complex binder interface in the binder stabilized preforms under consideration. Simulation models of forming of woven fabrics have been studied extensively in the literature [3,4]. However, models of UD-NCF have only sparsely been reported in the literature. Most simulation models of NCF are formulated at the meso-scale, where the stitches are modeled discretely [5,6]. Recently, homogenous macro scale models of UD-NCF have been proposed by e.g. [7]. Numerical models on forming of multilayered composites have been the subject for recent research [8–11]. Common for most simulation models of multilayered composites is that separation often is neglected, and sliding is modeled by frictional laws. Delamination may occur locally in a preform in compression due to fiber instabilities. A description of ply delamination is, therefore, needed to accurately predict fiber wrinkling. Recent literature also points out the need for characterizing the binder interface for choosing an optimal forming strategy and reducing manufacturing cost [12]. Previously, cohesive zone models have been used to predict delamination during creasing of paperboard material [13], and UD carbon fabric for automated fiber placement [14]. However, to the authors' knowledge, cohesive zone modeling has not previously been used to describe a binder interface in preforms.

The aim of the present paper is to present current state of a binder stabilized preform simulation model that can be used to simulate wrinkles created during forming. The proposed model uses a traction-separation law to describe deformation and degradation of the binder interface. Firstly, the preform material and the specific deformation modes of the preform are presented. After this follows a description of the proposed model which is then compared with a preform vacuum experiment. This paper concludes with a discussion on the predictive capabilities of the proposed model, together with a discussion on limitations of the model and model improvements for future work.

Preform Material

The preforms are made of stacked non-crimp fabrics consisting of unidirectional glass fibers (UD-NCF). The UD glass fibers are stabilized by a layer of backing fibers oriented at ±80˚. The UD-NCFs have an area weight of 1322 g/m^2, with a backing fiber weight percent of approximately 2wt%. The backing fibers are stitched to the UD fibers by a polyester thread in a tricot-chain like pattern. A polymeric binder is placed between the NCFs plies to ease the handling of the preform. The thickness of each UD-NCF ply is approximately 1 mm, and the preform is made of 16 stacked UD-NCF plies which gives the preform a total height of approximately 16 mm. The preforms are pre-consolidated under vacuum at elevated temperatures. The preform can be seen in Fig. 1, with indication of the local coordinate system.

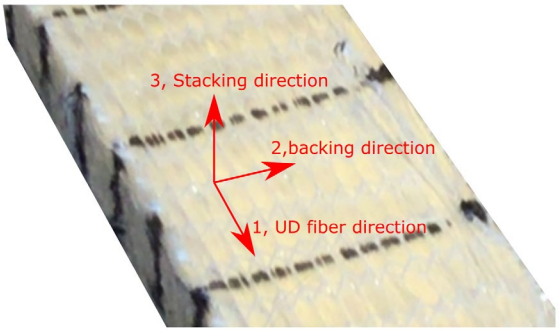

Fig. 1: Cut-out of binder stabilized preform. The preform is made of stacks of dry UD-NCFs that have been consolidated with a polymeric binder.

Numerical Simulation Model

A fiber-binder preform can be modeled at different length scales, see Fig. 2. At the micro-scale the fibers are assumed homogenous and modeled discretely. At meso-scale the fiber rovings are assumed homogenous, and the stitches of the NCF and the dispersed binder are modeled discretely. At macro-scale each UD-NCF ply is modeled separately as a homogenous material, and the binder interface is modeled homogenously. At structural-scale the whole preform is modeled as a homogenous continuum. For the present model it is desired to make a macro-scale model of the preform, as it offers low computational time compared to micro-, and meso-scale modeling. The macro-scale model still provides significant information on the inter-ply deformation (degradation of the binder interface) which a structural-scale model would not be able to describe.

When modeling the preform at macro-scale, the intra-ply interactions are neglected. This could be relative fiber sliding or deformation of stitching. Thus, it is important that the macro-scale model is capable of describing significant deformation modes arising from intra-ply deformations at lower scales. This can be achieved by selecting a proper material model accounting for the inherent anisotropy of the structure. For the present study an elastic orthotropic material model is used.

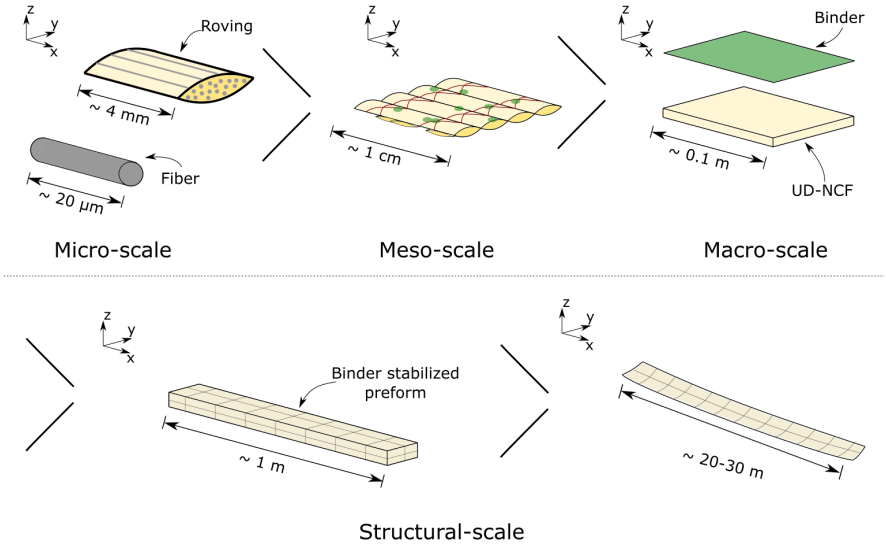

Fig. 2: Different modelling scales for a binder stabilized preform.

The present preform model is a 2D model in the 1-3 plane of the preform, see Fig. 1, which means that the effects of the preform width in the backing direction are neglected. In-plane shearing is not accounted for in this 2D model, which reduces the influence of the stitching geometry. In the 2D macro-scale model the deformation modes shown in Fig. 3 can be described. The in-plane deformation mode are elongation and compression of the UD-NCF plies. The plies have a high membrane tensile stiffness as the fibers will be in tension, whereas, the membrane compressive stiffness is low due to fiber instabilities. The out-of-plane deformation modes are bending, through thickness compaction and transverse shearing. The bending, compaction, and transverse shear stiffnesses of the UD-NCF are low due to relative fiber movement. Some permanent deformation is also expected for the out-of-plane modes due to friction between fibers and relative fiber motion. To describe the specific deformation modes of the UD-NCF at macro-scale, these should ideally be decoupled and described separately. The inter-ply deformation modes are ply separation and relative ply sliding. These two deformation modes correspond to mode-I and mode-II deformation from fracture mechanics. Both mode-I and mode-II delamination occurs during preform wrinkling.

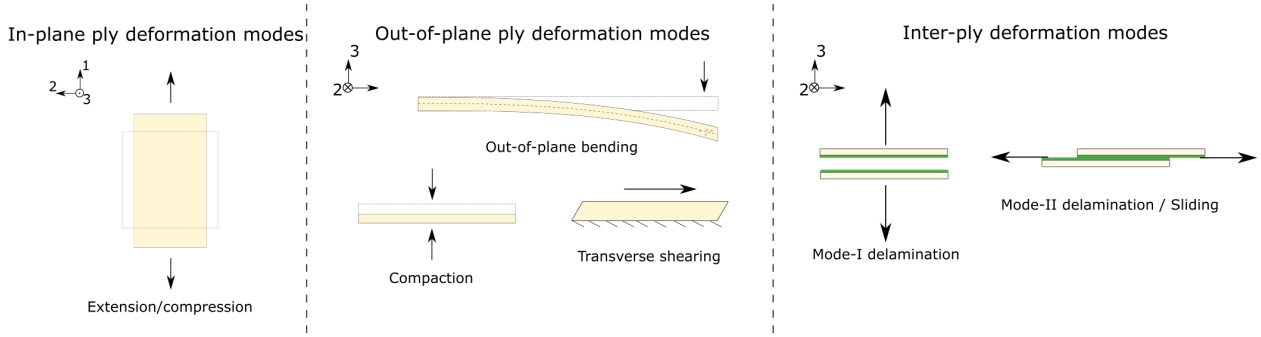

Fig. 3: Deformation modes for a macro-scale model of the preform.

The current 2D preform model is shown in Fig. 4. The model is desired to be based on commercially available finite element analysis (FEA) software. Each UD-NCF layer is modeled separately by solid continuum elements (C3D8R in ABAQUS) with linear elastic material properties, and the binder material is modeled as a cohesive interface. The use of solid elements improves the contact surface representation compared to shell elements with an offset. An orthotropic material model is used for the UD-NCFs. The model is constrained with plane stress boundary conditions, and is solved using ABAQUS/Explicit. To decrease computational time the preform is modeled with 8 layers of double thickness.

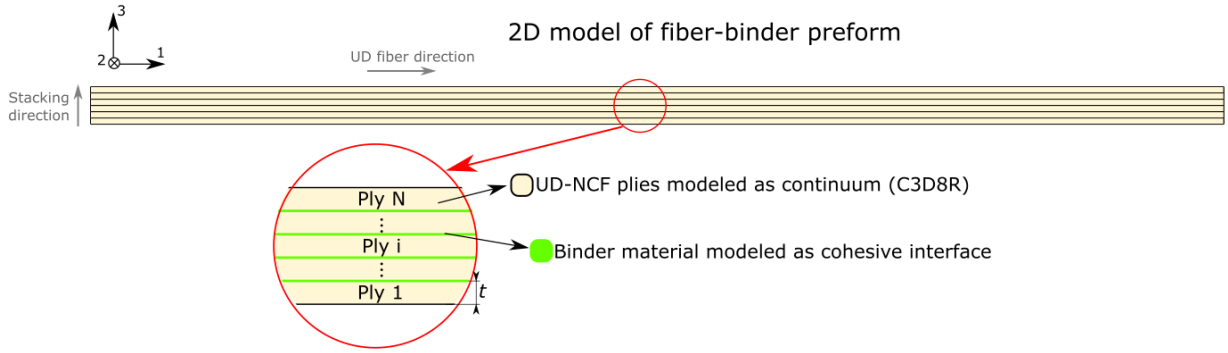

Fig. 4: Model of the fiber preform. Each UD-NCF ply is modeled separately as a continuum, and the interface between the plies are modeled as a cohesive interface.

A bilinear traction-separation law is used to describe the cohesive interface between the plies, see Fig. 5 (a). As wrinkle creation in the fiber preform involves mixed mode crack propagation, a mixed mode cohesive law is used, Fig. 6 (b).

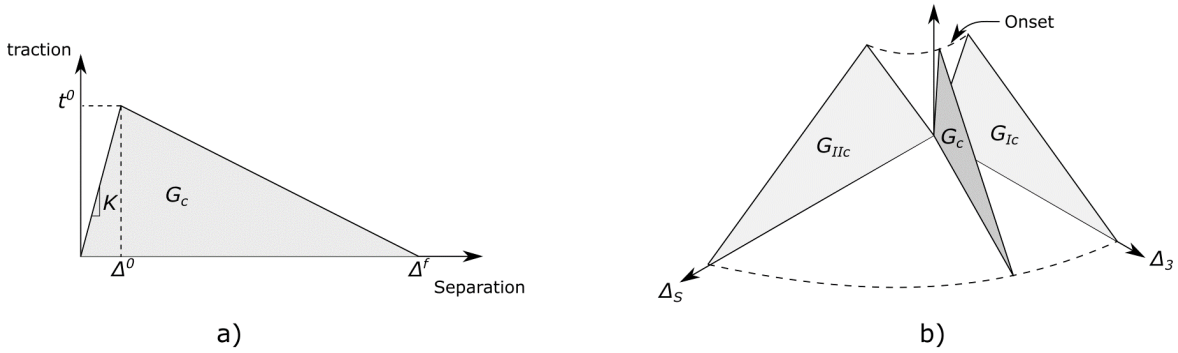

Fig. 5: Bilinear traction separation law (a), and a mixed mode cohesive law (b) used for modeling the binder interface.

For the onset of damage in the interface a maximum nominal stress criterion is used,

$$\max\left\{\frac{\langle t_3\rangle}{t_3^0}, \frac{t_2}{t_2^0}, \frac{t_1}{t_1^0}\right\} = 1. \tag{1}$$

In this criterion t_3 is the nominal tractions normal to the interface, and t_2 and t_1 are the shear stresses in both shear directions. Superscript 0 on the t denotes the onset traction of the i'th deformation mode. For damage propagation the critical energy release rate is used as criteria,

$$G = G_I + G_S \geq G_c. \tag{2}$$

Where $G_s = G_{II} + G_{III}$, and the critical energy release rate, G_c, is interpolated using the Benzeggagh-Kenane criterion [15],

$$G_c = G_{Ic} + (G_{IIc} - G_{Ic})B^{\eta}, \; B = \frac{G_S}{G_I + G_S}. \tag{3}$$

Characterization of Material Properties

The material properties needed as input to the model are membrane, transverse shear, and compaction stiffnesses of the plies, and traction-separation laws for mixed mode crack propagation of the binder interface. For the present study the bending stiffness of the UD-NCF plies and mode-I critical energy

release rate of the binder interface have been characterized by a cantilever bending test [16] and t-peel test, respectively, see Fig. 6. The fabric and binder are characterized as being homogenous i.e. the effect of stitches, binder dispersion etc. are implicitly accounted for in the characterized responses.

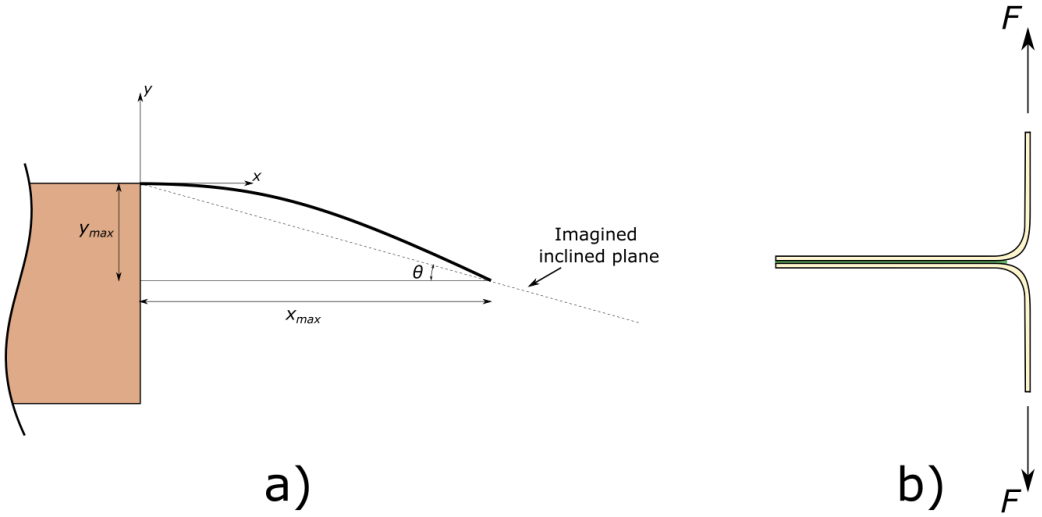

Fig. 6. Cantilever bending test used for obtaining a linear moment-curvature relationship (a). T-peel test used for obtaining the mode-I critical energy release rate of the binder interface (b).

Characterization of Bending Stiffness. The cantilever bending test is used to estimate the bending stiffness. In this test a piece of fabric is left to deform due to its own weight until it settles at a given deformation. The deflection of the fabric is measured by image processing similar to what is done in [17,18]. Based on the deflection curve, a constant stiffness D_{11} is estimated using Peirce's formula [17],

$$D_{11} = \frac{L^3}{8}\frac{\cos\theta/2}{\tan\theta}w,\ \theta = \frac{y_{max}}{x_{max}}. \tag{4}$$

where L is the length of the fabric being bent, θ is the angle of the inclined plane calculated by the endpoints of the deflection curve, and w is the area weight of the fabric. The stiffness of the plies is measured to $D_{11} = 50\text{Nmm}$. D_{11} is implemented in the orthotropic material model used for the UD-NCFs by setting $E_1 = \frac{12D_{11}}{t^3}$, where t is the thickness of the UD-NCFs. The calculated value of E_1 makes the UD-NCFs response in tension and compression unphysical as the membrane stiffness is affected. A fitted value of $E_1 = 6\text{GPa}$ is, therefore, used instead.

Characterization of Mode-I Fracture Toughness. To estimate the mode-I fracture toughness of the binder material t-peel tests have been conducted [19], see Fig. 6 b). In the t-peel test, two UD-NCF plies are being pulled apart at a fixed rate in a standard tensile test machine. The mode-I critical energy release rate is estimated by,

$$G_{IC} = \frac{2F}{b}. \tag{5}$$

where b is the width of the test specimen. The mode-I fracture toughness is measured to 160 J/m^2. As G_{IIc} is not characterized it is given the same value as G_{Ic} in the damage propagation criterion of Eq. (3).

Results

To test the performance of the simulation model it is compared with results from a real forming case of the fiber-binder preform structure.

Preform Vacuum Experiments. The vacuum experiments are carried out by placing a preform specimen on a wedge and applying vacuum. The initially straight preform is then formed over the wedge, see Fig. 7.

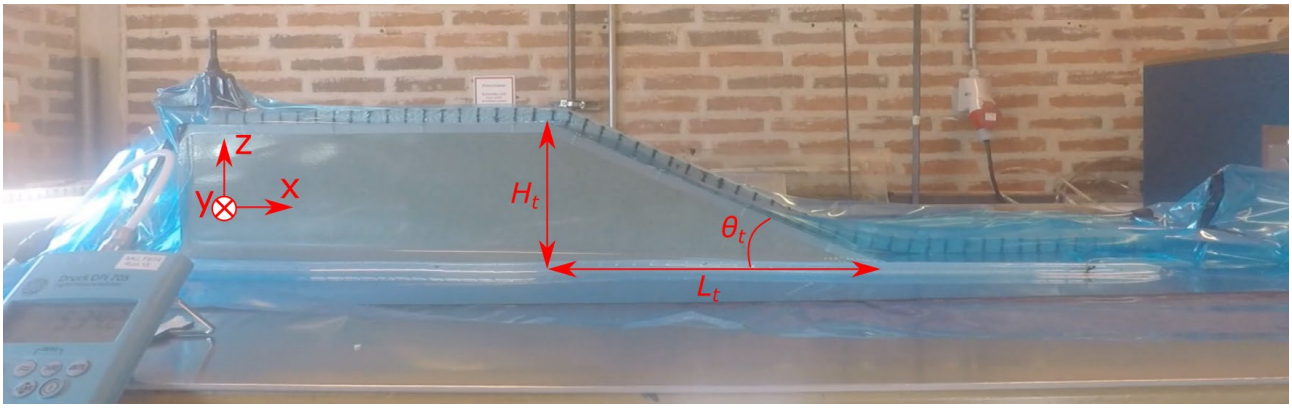

Fig. 7: Deformed configuration of the preform during the vacuum experiments. The initial straight preform is formed on the wedge.

The wedge being used have an angle of $\theta_t = 25°$ and a length of $L_t = 320$ mm. The preform specimens used for the experiments have dimensions [1000 mm x 50 mm] and full thickness.

Comparison of the Experiments with the Numerical Model. The comparison can be seen in Fig. 8. The comparison is done at three different locations on the preform; at the top transition, the shear region, and the bottom transition. At the top transition wrinkles facing down towards the mold are observed in the experiments. These wrinkles are also predicted by the model. The size of the wrinkle in the model is approximately 2 cm, whereas, the wrinkles observed in the experiments are approximately 1 cm. Delamination at the wrinkle sites are also predicted by the model, which is also observed in the experiments. In the shearing region the preform is undergoing transverse shearing in the experiments, with a shearing angle of approximately 6°. The simulation model predicts a transverse shear angle of approximately 1.5°. At the bottom transition a surface wrinkle of approximately 2 cm is observed in the experiments. The simulation model predicts a surface wrinkle at the same location with a size of 4 cm. The model predicts delamination at the wrinkle site which is also observed in the experiments.

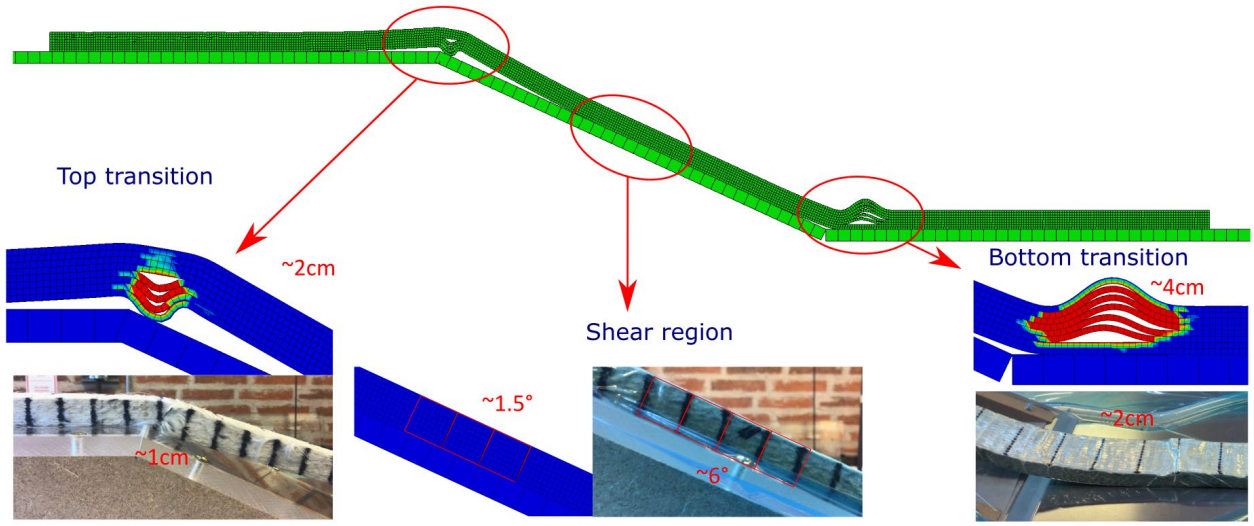

Fig. 8. Comparison of the deformed configuration of the preform from the simulation and the vacuum experiments. Red contours in the model indicate full damage of the binder interface.

Discussion

The model is capable of predicting the location and overall shape of the wrinkles arising during forming of the preform. In the experiments delamination of the binder interface is observed at the wrinkle sites, while no delamination is observed in the shear region. Both these phenomena are captured by the model. Wrinkles occurs in binder stabilized preforms due to a combination of binder delamination at wrinkle sites, and limited fiber sliding and binder deformation at shear regions.

The difference in wrinkle size is expected to be due to the bending stiffness being slightly higher in the model than in the UD-NCFs tested. The bending and membrane stiffness are not decoupled since solid elements with linear elastic material properties are used in the model. The membrane stiffness can therefore be chosen to either represent the estimated membrane or the estimated bending stiffness of the model. The former will result in a high bending stiffness which influences the size of the wrinkles. The latter will result in a low membrane stiffness which results in membrane deformation of the plies rather than wrinkling. The transverse shearing of the preform is underpredicted by the model. The overly high transverse shear stiffness of the model increases the compressive longitudinal stress in the fibers. This leads to out-of-plane deformation of the ply due to instability, which may result in larger wrinkles which initiates at an earlier stage in the forming process. However, since the modeled membrane stiffness of the UD-NCFs is relatively low (to account for the low bending stiffness of the plies without decoupling), the compressive longitudinal stresses may result in compressive deformation of the fibers rather than wrinkling. The mode-II critical energy release rate have not been characterized as input for the model. This will probably be higher than the mode-I critical energy release rate. A higher mode-II critical energy release rate may decrease the size of the wrinkles by limiting the propagation of initiated wrinkles. In the vacuum experiment the wrinkle creation is governed by forming rather than consolidation [20]. Furthermore, limited compaction occurs during the vacuum forming because the preforms are pre-consolidated. This means that the linear compaction stiffness used for the present model is sufficient for describing the compaction. If the model is to be used in a consolidation driven simulation, a non-constant compaction stiffness may need to be implemented [8].

The current model is made for 2D analysis of preform forming. To model forming over double curved geometric transitions, this model needs to be extended to include 3D deformation modes. The 2D model may be able to accurately model forming of wide preforms, if the transitions considered are not double curved, and plane strain assumptions are used.

Conclusion

In this paper a model for simulating forming of binder stabilized preforms using a cohesive traction-separation law for the binder interface is described. The model considers the UD-NCF plies as a homogenous continuum with a linear elastic orthotropic material model, and the binder material as a homogenous cohesive interface between the plies. The model can predict the location of the wrinkles arising during forming of binder stabilized preforms, and the binder delamination that occurs at the wrinkle sites. The size of the wrinkles predicted by the model is larger than observed in experiments. The reason is expected to be due to the bending and membrane stiffness not being decoupled in the present model. So far, only orthotropic linear elastic material models for the UD-NCFs is used. In future work the modeling framework will be extended to also include non-linear material models of the plies, as well as decoupling of the bending and the membrane stiffnesses. The enhanced model will thereby be able to accurately predict possible defects such that they can be dealt with before the production stage of the wind turbine blade

Acknowledgements

This study was completed as part of the MADEBLADES research project supported by the Energy Technology Development and Demonstration Program, Grant no. 64019-0514.

References

[1] J. J. Bender, S. R. Hallett, and E. Lindgaard, Investigation of the effect of wrinkle features on wind turbine blade sub-structure strength, Compos. Struct. 218 (2019) 39–49.

[2] C. Krogh *et al.*, A simple MATLAB draping code for fiber-reinforced composites with application to optimization of manufacturing process parameters, Struct. Multidiscipl. Optim 64 (2021) 457–471.

[3] P. Boisse, J. Huang, and E. Guzman-Maldonado, Analysis and modeling of wrinkling in composite forming, J. Compos. Sci. 5(3) (2021) 1–16.

[4] P. Harrison, M. F. Alvarez, and D. Anderson, Towards comprehensive characterisation and modelling of the forming and wrinkling mechanics of engineering fabrics, Int. J. Solids. Struct. 154 (2018) 2–18.

[5] S. Bel, N. Hamila, P. Boisse, and F. Dumont, Finite element model for NCF composite reinforcement preforming: Importance of inter-ply sliding, Compos. A: Appl. Sci. Manuf. 43(12) (2012) 2269–2277.

[6] G. Creech and A. K. Pickett, Meso-modelling of Non-crimp Fabric composites for coupled drape and failure analysis, J. Mater. Sci. 41(20) (2006) 6725–6736.

[7] F. J. Schirmaier, D. Dörr, F. Henning, and L. Kärger, A macroscopic approach to simulate the forming behaviour of stitched unidirectional non-crimp fabrics (UD-NCF), Compos. A: Appl. Sci. Manuf. 102 (2017) 322–335.

[8] J. P. H. Belnoue, O. J. Nixon-Pearson, A. J. Thompson, D. S. Ivanov, K. D. Potter, and S. R. Hallett, Consolidation-driven defect generation in thick composite parts, J. Manuf. Sci. Eng. 140(7) (2018).

[9] E. Guzman-Maldonado, P. Wang, N. Hamila, and P. Boisse, Experimental and numerical analysis of wrinkling during forming of multi-layered textile composites, Compos. Struct. 208 (2018) 213–223.

[10] A. J. Thompson, J. P. H. Belnoue, and S. R. Hallett, Modelling defect formation in textiles during the double diaphragm forming process, Compos. B: Eng. 202 (2020).

[11] K. Vanclooster, S. V. Lomov, and I. Verpoest, Simulation of multi-layered composites forming, Int. J. Mater. Form. 3 (2010) 695-698.

[12] F. Henning, L. Kärger, D. Dörr, F. J. Schirmaier, J. Seuffert, and A. Bernath, Fast processing and continuous simulation of automotive structural composite components, Compos. Sci. Technol. 171 (2019) 261–279.

[13] L. A. A. Beex and R. H. J. Peerlings, An experimental and computational study of laminated paperboard creasing and folding, Int. J. Solids. Struct. 46(24) (2009) 4192-4207.

[14] B. Durif, N. Moulin, S. Drapier, L. Bouquerel, and M. Blais, Challenges in modelling the forming of unidirectional HiTape® reinforcements, ESAFORM 2021, Liège, Belgium

[15] M. L. Benzeggagh and M. Kenane, Measurement of mixed-mode delamination fracture toughness of unidirectional glass/epoxy composites with mixed-mode bending apparatur, Compos. Sci. Technol. 56 (1996) 439–449.

[16] C. Krogh, P. H. Broberg, J. Kepler, and J. Jakobsen, Comprehending the bending: A comparison of different test setups for measuring the out-of-plane flexural rigidity of a UD fabric, ESAFORM 2022, Braga, Portugal

[17] E. de Bilbao, D. Soulat, G. Hivet, and A. Gasser, Experimental Study of Bending Behaviour of Reinforcements, Exp. Mech. 50(3) (2010) 333–351.

[18] B. Liang, P. Chaudet, and P. Boisse, Curvature determination in the bending test of continuous fibre reinforcements, Strain 53(1) (2017) 1–12.

[19] S. Schmidt, T. Mahrholz, A. Kühn, and P. Wierach, Powder binders used for the manufacturing of wind turbine rotor blades. Part 1. Characterization of resin-binder interaction and preform properties, Polym. Compos. 39(3) (2018) 708–717.

[20] M. Thor, M. G. R. Sause, and R. M. Hinterhölzl, Mechanisms of origin and classification of out-of-plane fiber waviness in composite materials — A review, J. Compos. Sci. 4(3) (2020).